dysfunction in obstructive sleep apnea syndrome by nasal continuous positive airway pressure--possible involvement of nitric oxide and asymmetric NG, NG-dimethylarginine. Circ J. 69: 221-6, 2005

土屋一洋

56) Arimura H, Li Q, Koroigi Y, Hirai T, Katsuragawa S, Yamashita Y, Tsuchiya K, Doi K. Computerized detection of intracranial aneurysms for three-dimensional MR angiography: Feature extraction of small protrusions based on a shape-based difference image technique. Med Phys 33: 394-400, 2006.

57)Hirai T, Korogi Y, Arimura H, Katsuragawa S, Kitajima M, Yamura M, Yamashita Y, Doi K. Intracranial aneurysms at MR angiography: effect of computer-aided diagnosis on radiologists' detection performance. Radiology 237:605-610, 2005.

58)Tsuchiya K, Honya K, Fujikawa A, Tateishi H, Shiokawa Y. Postoperative assessment of extracranial-intracranial bypass by time-resolved 3D contrast-enhanced MR angiography using parallel imaging. AJNR Am J Neuroradiol. 2005:26:2243-7.

勝谷友宏

59)Masuo K, Katsuya T, Fu Y, et al. Beta2- and beta3-adrenergic receptor polymorphisms are related to the onset of weight gain and blood pressure elevation over 5 years. Circulation. 2005;111(25):3429-3434.

60)Masuo K, Katsuya T, Fu Y, et al. Beta2-adrenoceptor polymorphisms relate to insulin resistance and sympathetic overactivity as early markers of metabolic disease in nonobese, normotensive individuals. Am J Hypertens. 2005;18(7):1009-1014.

61)Masuo K, Katsuya T, Kawaguchi H, et al. Rebound weight gain as associated with high plasma norepinephrine levels that are mediated through polymorphisms in the beta2-adrenoceptor. Am J Hypertens. 2005;18(11):1508-1516.

62)Iwashima Y, Katsuya T, Ishikawa K, et al. Association of hypoadiponectinemia with smoking habit in men. Hypertension. 2005;45(6):1094-1100.

武地 一

63)Sumi E, Takechi H, Wada T, Ishine M, Wakatsuki Y, Murayama T, Yokode

M, Tanaka M, Kita T, Matsubayashi K, and Arai H. Comprehensive geriatric assessment for outpatients is important for the detection of functional disabilities and depressive symptoms associated with sensory impairment as well as for the screening of cognitive impairment. Geriat Gerontol Int, in press

64)Nomura I, Takechi H, Kato N, Kita T. Inhibition of long term potentiation by amyloid beta is mediated in a mechanism independent of NMDA receptor or VDCC in hippocampal CA1 pyramidal neurons. 391, 1-6. 2005

65)Arai H, Takechi H, Wada T, Ishine M, Wakatsuki Y, Horiuchi H, Murayama T, Yokode M, Tanaka M, Kita T, Matsubayashi K, and Kume N. Usefulness of measuring serum markers in addition to comprehensive geriatric assessment for cognitive impairment and depressive mood in the elderly. Geriat Gerontol Int, in press

横手幸太郎

66)Yokote K, Kobayashi K and Saito Y.. Role of TGF-・/ Smad3 signaling in response to vascular injury. Trends Cardiovasc Med, In press

67)Honjo S, Yokote K, Takada A, Maezawa Y, Kobayashi K, Sonezaki K, Saito Y. Etidronate ameliorates painful soft tissue calcification in Werner syndrome. J Am Geriat Soc 53:2038-2039, 2005

68)Kobayashi K, Yokote K, Fujimoto M, Yamashita K, Sakamoto A, Kitahara M, Kawamura H, Maezawa Y, Asaumi S, Tokuhisa T, Mori S, Saito Y. Targeted disruption of TGF-β-Smad3 signaling leads to enhanced neointimal hyperplasia with diminished matrix deposition in response to vascular injury. Circ Res (Cover article) 96: 904-912, 2005

和文原著、著書

主任研究者

鳥羽研二

1)鳥羽研二：2.老化の理解と活き活き長寿. 日老医誌 43(1)；65～67, 2006. Jan

2)東間紘, 出席者山口脩, 井上裕美, 鳥羽研二：頻尿・尿失禁―中高年の明るい過ごし方―. カレントテラピー 24(1)；90～96, 2006. Jan

3)鳥羽研二：老化度の測定. 新・老化学 第6章；111～124, 2005.

4)鳥羽研二：排尿障害にどうアプローチするか. 治療学 39(11)；1231～1242, 2005. Nov

5)鳥羽研二：高齢者の排尿障害を巡る問題. 治療学 39(11)；1191～1195

, 2005. Nov
6)鳥羽研二：高齢者高血圧治療とＡＲＢの可能性―高齢者高血圧における至適血圧と臓器保護を考える―. Ther. Res. 26(10) 1945¯1953, 2005. Oct
7)鳥羽研二：高齢者医療の実情に合った評価法を確立. 性差と医療 2(7)；793～795, 2005. Jul
8)鳥羽研二：介護予防，考え方と問題点 介護保険制度の見直しにあたって. 日老医誌 42(4)；383～391, 2005. Jul
9)馬場 幸，寺本信嗣，長谷川浩，町田綾子，秋下雅弘，鳥羽研二：痴呆高齢者に対する嚥下障害のスクリーニング方法の検討：簡易嚥下誘発試験と反復唾液嚥下テストの比較. 日老医誌 42(3)；323～327, 2005. May
10)鳥羽研二，大河内二郎，高橋 泰，松林公蔵，西永正典，山田思鶴，高橋龍太郎，西島令子，小林義雄，町田綾子，秋下雅弘，佐々木英忠：転倒者ハイリスク者の早期発見の評価方法作成ワーキンググループ：転倒リスク予測のための「転倒スコア」の開発と妥当性の検証. 日老医誌 42(3)；346～352, 2005. May
11)大内尉義，寺本信嗣，鳥羽研二，秋下雅弘，長野宏一郎，江頭正人，須藤紀子，井藤英喜，井上聡，梅田祐美：臨床医学の展望 老年医学. 日本醫事新報 4223, 2005. Apr
12)鳥羽研二：高齢者総合的機能評価とは. Geriat. Med. 43(4)；549～552, 2005. Apr
13)鳥羽研二：老年症候群，転倒寝たきり予防のために. 精神経誌 107(4)；354～358, 2005. Apr

分担研究者
森本茂人

14)中橋 毅、森本茂人：８．骨・関節 ２．骨粗鬆症. 予防とつきあい方シリーズ 老年病・認知症～長寿の秘訣～監修 荻原俊男 ﾒﾃﾞｨｶﾙﾋﾞｭｰ社 153-154, 2006
15)中橋 毅、森本茂人：８．骨・関節 １．老化にともなう骨の変化と病気. 予防とつきあい方シリーズ 老年病・認知症～長寿の秘訣～監修 荻原俊男 ﾒﾃﾞｨｶﾙﾋﾞｭｰ社 151-152, 2006
16)森本茂人：第 3 章 現代社会と疾病. Ⅰ.老人性疾患 新版 介護福祉士養成講座 医学一般（福祉士養成講座編集委員会）中央法規出版㈱40-51, 2005
17)森本茂人：副甲状腺機能亢進症、副甲状腺機能低下症、無症候性副甲状腺機能亢進症. 最新医学大辞典第３版（医歯薬出版編）医歯薬出版㈱1601, 1795, 2005
18)中橋 毅、森本茂人、松本正幸：第Ⅲ編 高齢のお客様・障害のあるお客様の理解と接客・援助 第１章「高齢のお客様への接客・援助」. ﾊｰﾄﾌﾙ美容師養

成研修用ﾃｷｽﾄ　中央法規出版㈱61-103，2005
19)森本茂人：高血圧　高齢者の安全な薬物療法ｰｶﾞｲﾄﾞﾗｲﾝ2005ｰ．ﾒﾃﾞｨｶﾙﾋﾞｭｰ社　86-105，2005

岩本俊彦
20)岩本俊彦：心疾患・呼吸器疾患に関連した神経障害：呼吸器疾患．CLINICAL NEUROSCIENCE 24：90-91，2006.
21)岩本俊彦：臨床老年医学：上巻：診断と評価編．ライフ・サイエンス、東京、2005.
22)岩本俊彦：手足のしびれ．老年病ガイドブック1（鳥羽研二編）、メジカルビュー、東京、2005、pp138-145.
23)岩本俊彦：脳血管性痴呆の診断．老年病ガイドブック4（三木哲郎編）、メジカルビュー、東京、2005、pp120-128.
24)岩本俊彦：老年医学からみた脳病変におけるリポ蛋白(a)の臨床的意義．東医大雑誌 63：3-8，2005.
25)岩本俊彦：痴呆性疾患の診療と介護：「物忘れ外来」の現状と効果．臨床と研究 82：77-80，2005.
26)岩本俊彦、中井利紀、木村明裕、平尾健太郎：高度白質病変例の血小板凝集能とその予後．脈管学 45：951-957，2005.
27)岩本俊彦：総説：維持透析患者の閉塞性動脈硬化症に併発する脳血管障害．クリニカルエンジニアリング別冊：維持透析患者の閉塞性動脈硬化症（阿岸鉄三編）、秀潤社、東京、2005、pp52-61.
28)岩本俊彦：特集：アルツハイマー病-脳血管性痴呆の診断、治療、予防．日本医師会雑誌 134:1017-1021，2005.
29)岩本俊彦：増加する心原性脳塞栓症、その予防と治療．日老医誌 42：504-507，2005.
30)岩本俊彦：痴呆-アルツハイマー型痴呆を中心として：医学と薬学 53:311-321，2005.
31)宮路裕子、櫻井博文、黄川田雅之、岩本俊彦：褥瘡治療に関する研究-実験計画法による組み合わせ治療．日老医誌 42：90-98，2005.
32)岩本俊彦、木村明裕、中井利紀：アルツハイマー病の合併症と対策-転倒・嚥下障害．Modern Physician 25:1124-1127，2005.
33)岩本俊彦：特集＝高齢者診療の話題-多発性脳塞栓症．Medicament News 1847：1-3，2005.
34)岩本俊彦、櫻井博文：もの忘れ外来-診断の進め方と治療・ケア．日本醫事新報 4233:13-19，2005.

葛谷雅文

35)榎裕美、加藤昌彦、葛谷雅文、井澤幸子、岡田希和子、井口明久．在宅要介護高齢者における栄養指導 ADL との関連．栄養と評価 22 607-610, 2006

36)平川仁尚、益田雄一郎、葛谷雅文、大頭信義、梁勝則、井口明久、植村和正．高齢者の在宅終末期ケアに関する前向き研究．ホスピスケアと在宅ケア (Hospice and Home Care) 別冊 13 (3) 220-224, 2005

37)平川仁尚，益田雄一郎，植村和正，葛谷雅文，木股貴哉，井口昭久．癌告知および脳死・臓器移植に関する名古屋大学医学部 5 年生の意識調査．医学教育 36：187-192, 2005

38)平川仁尚、益田雄一郎、上村和正、葛谷雅文、野口美和子、木俣貴哉、井口昭久．全国の医学科・看護科における終末期医療・看護教育の実態調査．日老医誌 42: 540-545

39)葛谷雅文、大西丈二、井口昭久　高齢者医療の現場における低栄養ならびに栄養管理に認知度の調査 日本臨床栄養学会誌　26:235-238, 2005

神崎恒一

40)花岡陽子，山本寛，飯島勝矢，大賀栄次郎，神崎恒一，大内尉義：原因不明の発熱で発症し，赤芽球癆が先行した高齢者悪性リンパ腫の 1 例．日老医誌 42: 444-449, 2005

武地　一

41)杉原百合子、山田裕子、武地　一：一般高齢者のもつアルツハイマー型痴呆症についての知識量と関連要因の検討．日本認知症ケア学会誌　4 巻 1 号 Page 9-16, 2005

42)武地　一、山田裕子、杉原百合子、北　徹：もの忘れ外来通院中のアルツハイマー型痴呆症患者における行動・心理学的症候と認知機能障害、介護負担感の関連について．日本老年医学会雑誌　第４３巻２号

43)武地　一：センター方式の評価と今後の課題-医療の立場から一．介護支援専門員　7 巻 5 号　39-42, 2005

44)武地　一：高齢者医療における総合的機能評価（ＣＧＡ）．ファルマシア　41 巻 10 号　937-941, 2005

横手幸太郎

45)小林一貴，横手幸太郎，齋藤康：増殖因子とその受容体-PDGF, TGF-β-．柏木厚典．糖尿病カレントライブラリー③ 糖尿病と動脈硬化．文光堂：55-59, 2005

46)横手幸太郎：Werner 症候群．寺本民生・片山茂裕．講義録 内分泌・代謝学．

メディカルレビュー社：385-387，2005
47)横手幸太郎，齋藤康：インスリンと血管平滑筋細胞．日本糖尿病学会．糖尿病学の進歩．診断と治療社：215-216，2005

Available online at www.sciencedirect.com
SCIENCE DIRECT®
Clinica Chimica Acta 364 (2006) 328 – 334
www.elsevier.com/locate/clinchim

Angiotensin converting enzyme inhibitor attenuates oxidative stress-induced endothelial cell apoptosis via p38 MAP kinase inhibition

Wei Yu [a], Masahiro Akishita [b,*], Hang Xi [a], Kumiko Nagai [a], Noriko Sudoh [a], Hiroshi Hasegawa [a], Koichi Kozaki [a], Kenji Toba [a]

[a] Department of Geriatric Medicine, Kyorin University School of Medicine, Tokyo, Japan
[b] Department of Geriatric Medicine, Graduate School of Medicine, University of Tokyo, 7-3-1 Hongo, Bunkyo-ku, Tokyo 113-8655, Japan

Received 11 May 2005; received in revised form 22 July 2005; accepted 29 July 2005
Available online 8 September 2005

Abstract

Background: The effects of angiotensin converting enzyme (ACE) inhibitors on oxidative stress-induced apoptosis of endothelial cells and the intracellular signaling were investigated.
Methods: Cultured endothelial cells derived from a bovine carotid artery were treated with H_2O_2 or TNF-α to induce apoptosis. Apoptosis was evaluated by DNA fragmentation and cell viability, p38 MAP kinase activity by Western blotting, and oxidative stress by formation of 8-isoprostane. The effects of ACE inhibitors were examined by adding them into the medium throughout the experiments.
Results: Apoptosis was attenuated by ACE inhibitors, temocapril and captopril, in a dose-dependent manner (1–100 μmol/l). H_2O_2 (0.2 mmol/l for 1.5 h) or TNF-α (10 ng/ml for 72 h) treatment stimulated the activities of p38 MAP kinase. Temocapril and captopril decreased the activity of p38 MAP kinase as well as 8-isoprostane formation induced by H_2O_2. A p38 MAP kinase inhibitor, SB203580, partially inhibited the effect of temocapril on apoptosis.
Conclusions: These results suggest that ACE inhibitors protect endothelial cells from oxidative stress-induced apoptosis, and that p38 MAP kinase plays a critical role in the process.

Keywords: Apoptosis; ACE inhibitor; Endothelial cell; p38 MAP kinase

1. Introduction

Stress-induced injury of vascular endothelial cells (ECs) is considered to be an initial event in the development of atherosclerosis [1]. In particular, oxidative stress has been implicated in endothelial injury caused by oxidized LDL and smoking as well as hypertension, diabetes and ischemia-reperfusion [1–3]. This notion is supported by the findings that the production of reactive oxygen species is upregulated in vascular lesions [4,5], and that lesion formation such as endothelial dysfunction is accelerated by superoxide anion [6] and, in contrast, is attenuated by free radical scavengers including vitamin E [7] and superoxide dismutase [8].

Angiotensin converting enzyme (ACE) inhibitors effectively interfere with the renin angiotensin system and exert various beneficial actions on vascular structure and function beyond their blood pressure-lowering effects [9,10]. ACE inhibitors attenuate neointimal formation after vascular injury in animals [11] and endothelial dysfunction in humans [12]. It has been demonstrated that ACE activation induces oxidative stress [13]. However, it has not been elucidated whether ACE inhibitors could attenuate oxidative stress-induced EC apoptosis, an initial and important process in atherosclerosis [14,15].

In this study, we examined the effects of ACE inhibitors, temocapril and captopril, on H_2O_2- and TNF-α-induced EC apoptosis and the pro-apoptotic intracellular signaling, p38 mitogen-activated protein (MAP) kinase, to clarify the underlying mechanism.

* Corresponding author. Tel.: +81 3 5800 8832; fax: +81 3 5800 8831.
E-mail address: akishita-tky@umin.ac.jp (M. Akishita).

0009-8981/$ - see front matter © 2005 Elsevier B.V. All rights reserved.
doi:10.1016/j.cca.2005.07.021

2. Materials and methods

2.1. Induction of EC apoptosis

ECs derived from a bovine carotid artery [16] was cultured in Dulbecco's modified Eagle medium (Gibco) supplemented with 10% fetal bovine serum. Cells were maintained at 37 °C in a 95% air/5% CO_2 atmosphere. ECs of the 5th to 7th passage were used in the experiments. When the cells had grown to 70–80% confluence, ECs were pretreated for 24 h with culture medium containing the reagents that were tested in the experiments. Subsequently, after washing twice with Hank's balanced salt solution (Gibco), the cells were exposed to H_2O_2 (0.1–0.4 mmol/l) diluted in Hank's balanced salt solution for 1.5 h at 37 °C to induce apoptosis. The cells were washed three times with Hank's balanced salt solution, and then cultured in culture medium containing the reagents until assay. Similarly, tumor necrosis factor-α (TNF-α, 5-20 ng/ml; Sigma) was added to the medium until assay after 24-h pretreatment with the reagents tested. EC viability and apoptosis were evaluated at 24 h after H_2O_2 treatment, or at 72 h after TNF-α treatment. The effects of temocapril (1–100 μmol/l) and captopril (1–100 μmol/l) were examined by adding them into the medium throughout the experiments. The effect of a specific p38 MAP kinase inhibitor, SB203580 (10 μmol/l; Calbiochem), was examined by treating ECs with SB203580 for 1 h before H_2O_2 treatment.

2.2. Cell viability

Cell viability was estimated using an MTT (3-(4,5-dimethylthiazol-2-yl)-2,5-diphenyltetrazolium bromide; Sigma) assay [17]. Briefly, 1 mg/ml MTT (final concentration) was added to the well and incubated for 2 h at 37 °C. The medium was removed and cells were lysed with 2-isopropanol containing 0.04 mol/l HCl. The absorbance measured at 595 nm was used to calculate the relative cell viability ratio.

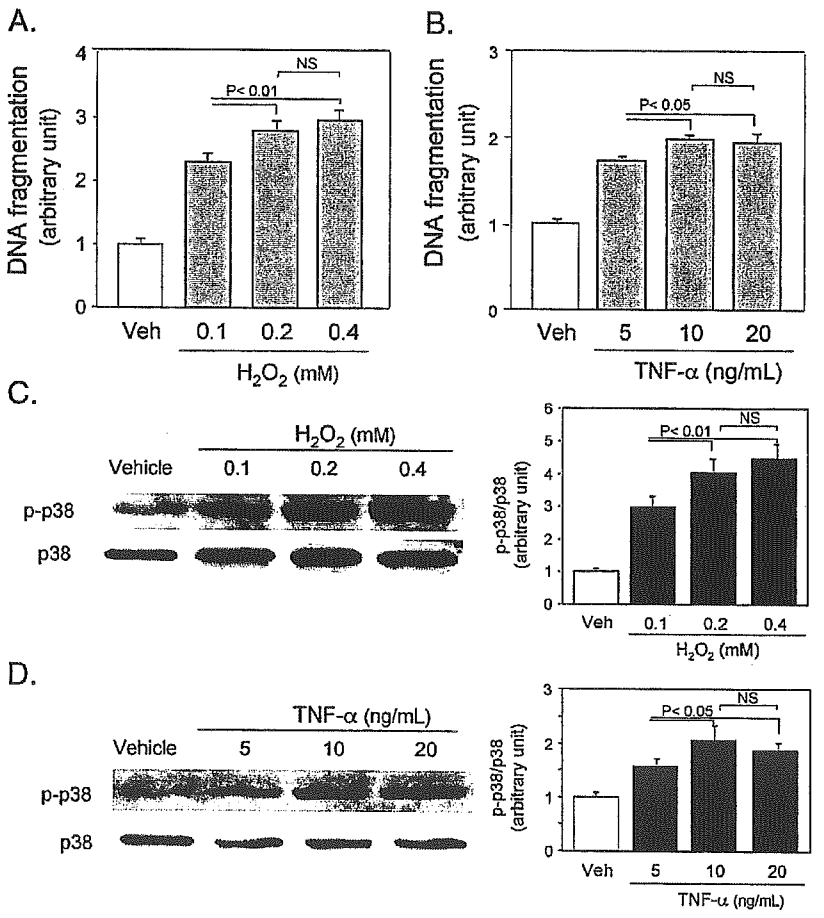

Fig. 1. Dose-dependent effects of H_2O_2 (A, C) and TNF-α (B, D) on EC apoptosis (A, B) and p38 MAP kinase activity (C, D). A and B, apoptosis was evaluated 24 h after H_2O_2 treatment (for 1.5 h) or 72 h after addition of TNF-α by means of DNA fragmentation ($n=3$). C and D, the activity of p38 MAP kinase was evaluated by immunoblotting using the specific antibody against the phosphorylated form of the kinase (p-p38) at 30 min after addition of H_2O_2 or TNF-α. Right panels show the results of densitometric analyses of immunoblotting (mean±SEM, $n=3$). NS, not significant. Values are expressed as mean±SEM ($n=3$).

2.3. Evaluation of EC apoptosis and formation of 8-isoprostane

For quantitative determination, EC apoptosis was measured as DNA fragmentation. DNA fragmentation was evaluated by histone-associated DNA fragments using a photometric enzyme immunoassay (Cell Death Detection ELISA, Roche), according to the manufacturer's instructions. Briefly, attached cells were harvested with trypsin, and the cell suspension was pelleted by centrifugation. Floating and attached cells were lysed. After centrifugation, the supernatant was measured by ELISA.

Formation of 8-isoprostane (8-*iso* prostaglandin $F_{2\alpha}$) was measured using a commercially available EIA kit (Cayman Chemical). Culture supernatants were diluted with EIA buffer when necessary, and were applied to EIA according to the manufacturer's instructions.

2.4. Immunoblotting

The cells were washed twice with ice-cold phosphate-buffered saline and lysed in lysis buffer (25 mmol/l Tris/HCl, pH 7.5, 25 mmol/l NaCl, 0.5 mmol/l EGTA, 10 mmol/l NaF, 20 mmol/l β-glycerophosphate, 1 mmol/l Na_3VO_4, 1 mmol/l

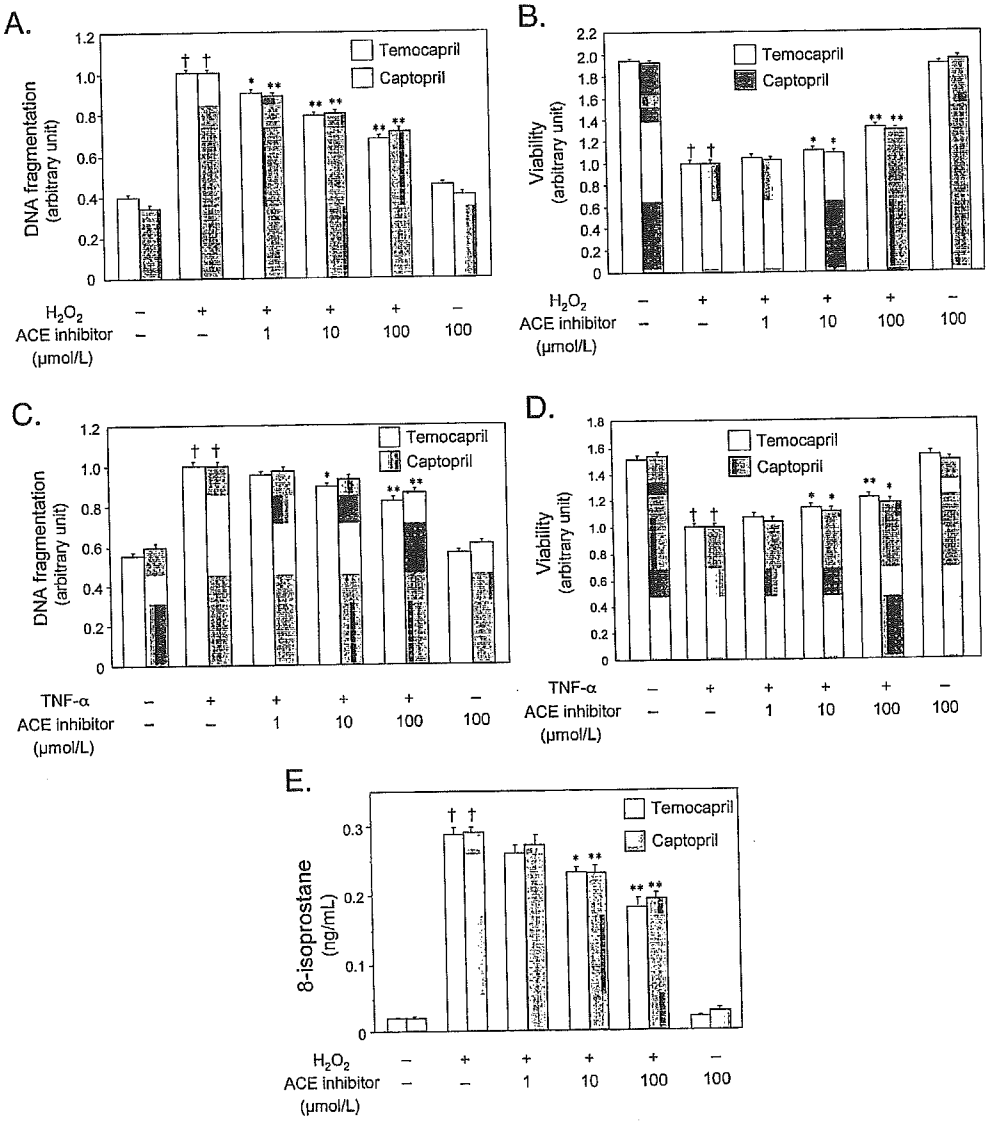

Fig. 2. Effects of ACE inhibitors on H_2O_2-induced (A, B) and TNF-α-induced (C, D) EC apoptosis and the effects of ACE inhibitors on H_2O_2-induced 8-isoprostne formation (E). Temocapril, captopril or their vehicle was added to the culture medium 24 h before H_2O_2 or TNF-α treatment until assay. Apoptosis (A, C) and cell viability (B, D) were evaluated 24 h after H_2O_2 treatment (0.2 mmol/l for 1.5 h) or 72 h after TNF-α treatment (10 ng/ml for 72 h) by means of DNA fragmentation ($n=3$) and MTT assay ($n=8$), respectively. 8-Isoprostane concentration (E; $n=3$) in the culture supernatant was measured 3 h after H_2O_2 treatment. A and B, †$P<0.01$ vs. H_2O_2 (−). *$P<0.05$, **$P<0.01$ vs. H_2O_2 (+)+ACE inhibitor (−). C and D, †$P<0.01$ vs. TNF-α (−). *$P<0.05$, **$P<0.01$ vs. TNF-α (+)+ACE inhibitor (−). Values are expressed as mean±SEM. Similar results were obtained in three independent experiments.

PMSF, and 10 μg/ml aprotinin) at 4 °C. After sonication and centrifugation at 15,000 rpm, the supernatant was used for the following immunoblotting. The lysate (20 μg protein per lane) was separated on 12% SDS-polyacrylamide gel, electroblotted onto nitrocellulose membrane, and immunoblotted with specific primary antibodies, both of which were purchased from Cell Signaling Technology (Beverly, MA). The antibodies used in this study were anti-phospho-p38 MAP kinase (phospho-p38 28B10 #9216) and anti-p38 MAP kinase (#9212). Antibodies were detected by means of a horseradish peroxidase-linked secondary antibody using an enhanced chemiluminescence system (Amersham Pharmacia Biotech). Densitometric analysis was performed using an image scanner and analyzing software (NIH image ver. 1.61). The activity of each kinase was evaluated by calculating the ratio of the amount of the phosphorylated form to that of the total form.

2.5. Data analysis

The values are expressed as mean±SEM in the text and figures. Data were analyzed using one-factor ANOVA. If a statistically significant effect was found, Newman–Keuls' test was performed to isolate the difference between the groups. Differences with a value of $P<0.05$ were considered statistically significant.

3. Results

3.1. Dose-dependent effects of H_2O_2 and TNF-α on EC apoptosis and p38 MAP kinase activity

Increasing concentrations of H_2O_2 and TNF-α were applied to examine the effects on EC apoptosis and p38 MAP kinase activity. Based on the literature [18] and time–response experiments (data not shown), EC apoptosis was evaluated at 24 h after H_2O_2 treatment for 1.5 h, or at 72 h after addition of TNF-α. The activity of p38 MAP kinase, as measured by immunoblotting using the specific antibody against the phosphorylated form of the kinase, was evaluated at 30 min after addition of H_2O_2 or TNF-α, based on time–response experiments (data not shown). As shown in Fig. 1A–D, the effects of H_2O_2 and TNF-α were

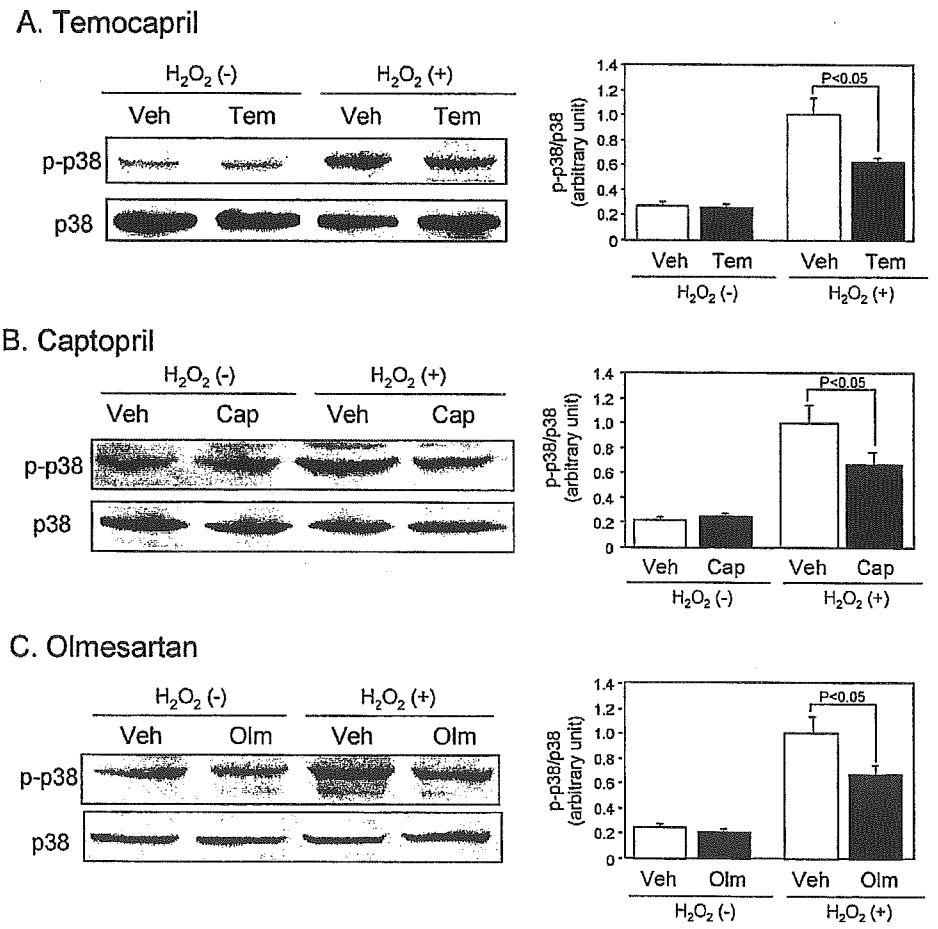

Fig. 3. Effects of temocapril (A), captopril (B) and olmesartan (C) on p38 MAP kinase activity at 30 min after exposure to H_2O_2. Temocapril (100 μmol/l), captopril (100 μmol/l), olmesartan (10 μmol/l) or its vehicle was added to the culture medium 24 h before H_2O_2 treatment until assay. Right panels show the results of densitometric analyses of immunoblotting (mean±SEM, $n=3$).

dose dependent, but there was no significant further increase in EC apoptosis and p38 MAP kinase activity by H_2O_2 of >0.2 mmol/l or by TNF-α of >10 ng/ml. Based on these data, the following experiments were examined using 0.2 mmol/l H_2O_2 or 10 ng/ml TNF-α.

3.2. Effect of ACE inhibitors on EC apoptosis

EC apoptosis, as measured by DNA fragmentation, was significantly attenuated by temocapril and captopril in a dose-dependent manner (Fig. 2A). Reflecting this effect, cell viability was ameliorated by addition of temocapril and captopril in a dose-dependent manner (Fig. 2B).

We also tested using TNF-α whether anti-apoptotic effects of ACE inhibitors would be specific to H_2O_2 or not. As shown in Fig. 2C, both temocapril and captopril effectively inhibited EC apoptosis in a dose-dependent manner. This was associated with the recovery of cell viability by the ACE inhibitors (Fig. 2D). Throughout the experiments, the effects of temocapril were comparable to those of captopril.

To confirm the antioxidant effects of temocapril and captopirl, the formation of 8-isoprostane, a marker of oxidative stress, was measured. Temocapril and captopril restrained 8-isoprostane formation induced by H_2O_2 in a dose-dependent manner (Fig. 2E).

3.3. Effect of ACE inhibitor on p38 MAP kinase activity

Next, the effects of ACE inhibitors on p38 MAP kinase activity were examined because the kinase has been implicated in the cell signaling leading to apoptosis [14,19,20]. As shown in Fig. 3A,B, temocapril and captopril decreased the activity of p38 MAP kinase at 30 min after H_2O_2 treatment by approximately 30–40% without any change in the total protein. An AT1 receptor blocker, olmesartan, showed similar effects on p38 MAP kinase activity (Fig. 3C).

Finally, the effect of a p38 MAP kinase inhibitor, SB203580, was examined. SB203580 reduced H_2O_2-induced EC apoptosis by 20%. More importantly, SB203580 partially but significantly inhibited the effect of temocapril on apoptosis (Fig. 4). Taking these results together with the pro-apoptotic action of p38 MAP kinase, it is suggested that p38 MAP kinase is involved in the effect of temocapril on EC apoptosis.

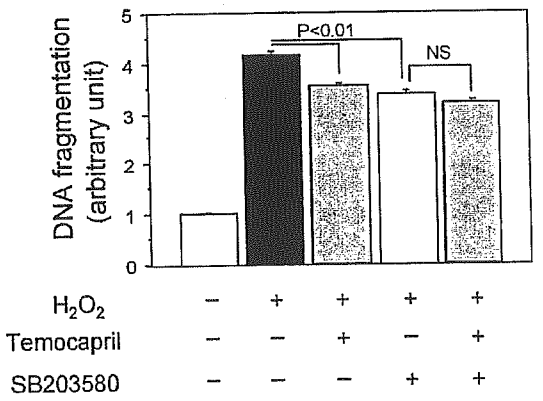

Fig. 4. Effects of temocapril and SB203580 on H_2O_2-induced EC apoptosis. Temocapril (100 μmol/l) or its vehicle was added to the culture medium 24 h before H_2O_2 treatment until assay. SB203580 (10 μmol/l) or its vehicle was added to the culture medium for 1 h before H_2O_2 treatment. EC apoptosis was determined by DNA fragmentation 24 h after H_2O_2 treatment. NS, not significant. Values are expressed as mean±SEM (n=3). Similar results were obtained in three independent experiments.

4. Discussion

A number of investigations have shown that angiotensin II induces oxidative stress in ECs. Angiotensin II stimulates the production of reactive oxygen species in ECs by upregulating the subunits of NAD(P)H oxidase, gp91 phox [21] and p47 phox [22]. It has been reported that the renin angiotensin system contributes to endothelial dysfunction in patients with renovascular hypertension [23]. Conversely, it has been shown experimentally that ACE inhibitors can reduce the production of reactive oxygen species in pathological conditions such as peripheral arteries in rats with chronic heart failure [24], rat diabetic nephropathy [25] and kidney mitochondria in aged rats [26]. In the clinical setting, 4-week treatment with ramipril, in patients with coronary artery disease, diminished the response of endothelium-dependent vasodilation to intracoronary administration of antioxidant vitamin C in parallel with improvement of basal endothelium-dependent vasodilation [27], indicating that ACE inhibitors can improve endothelial function in association with a reduction of oxidative stress.

In the present study, we investigated EC apoptosis, an important process that leads to endothelial dysfunction and atherosclerosis [14,15], and showed that ACE inhibitors, temocapril and captopril, attenuated EC apoptosis induced by H_2O_2 as well as by TNF-α. This result indicates that anti-apoptotic effects of ACE inhibitors are not specific to H_2O_2, but might be attributable to the anti-oxidant action of ACE inhibitors, because reactive oxygen species are known to be involved in TNF-α-induced EC apoptosis [28,29]. Reduction in 8-isoprostane formation by temcapril and captopril further supports the anti-oxidant effects of ACE inhibitors. It is not likely that the anti-apoptotic effects of ACE inhibitors were mediated through nitric oxide production via the inhibition of bradykinin degradation [11], because a nitric oxide synthase inhibitor, N^G-nitro-L-arginine methyl ester, did not influence the effect of temocapril on EC apoptosis (data not shown). Rather, the effects of ACE inhibitors are likely to be mediated through inhibition of angiotensin II production, as was demonstrated by the effect of olmesartan on p38 MAP kinase.

Reactive oxygen species activate many kinds of intracellular signaling, resulting in the transcription of numerous genes and the modulation of cellular function [30]. As

previously reported [31–33], extracellular signal-regulated kinase (ERK), c-Jun N-terminal kinase (JNK) and Akt in addition to p38 MAP kinase were activated in ECs by exposure to H_2O_2 (data not shown). Of these serine/threonine kinases, we focused on p38 MAP kinase because p38 MAP kinase is pro-apoptotic signaling, while ERK and Akt are anti-apoptotic, and JNK is anti- or pro-apoptotic depending on conditions [14,19,20]. We found that both temocapril and captopril inhibited the activity of p38 MAP kinase induced by H_2O_2. Although p38 MAP kinase is activated by stress and cytokines and acts on various target proteins, little is known about the downstream signaling [19,20,34]. However, EC apoptosis was effectively blocked in studies using a p38 MAP kinase inhibitor [35,36] and a dominant-negative form of p38 MAP kinase [35], indicating that activation of p38 MAP kinase leads to EC apoptosis. As a matter of fact, a p38 MAP kinase inhibitor, SB203580, partially inhibited H_2O_2-induced EC apoptosis in the present study. More importantly, SB203580 partially but significantly inhibited the effect of temocapril on apoptosis, further implying the role of p38 MAP kinase in the effect of temocapril. However, the partial effects of SB203580 also suggest the role of other pathways than p38 MAP kinase. We should perform future studies to determine the exact mechanism underlying H_2O_2-induced EC apoptosis.

In summary, we found that ACE inhibitors attenuated oxidative stress-induced EC apoptosis in culture. Furthermore, it was suggested that p38 MAP kinase was critical in the inhibitory effect of temocapril on EC apoptosis. These findings provide a mechanistic insight into the effects of ACE inhibitors, which have been used for the treatment of cardiovascular disease.

Acknowledgements

We thank Ms. Mariko Sawano for her excellent technical assistance. This study was supported by a Grant-in-Aid for Scientific Research from the Ministry of Education, Science, Culture and Sports of Japan (13670741), and by Health and Labour Sciences Research Grants (H16-Choju-013 and H16-Choju-015) from the Ministry of Health, Labour and Welfare of Japan.

References

[1] Ross R. Atherosclerosis—an inflammatory disease. N Engl J Med 1999;340:115–26.
[2] Griendling KK, Sorescu D, Lassegue B, Ushio-Fukai M. Modulation of protein kinase activity and gene expression by reactive oxygen species and their role in vascular physiology and pathophysiology. Arterioscler Thromb Vasc Biol 2000;20:2175–83.
[3] Zalba G, San Jose G, Moreno MU, et al. Oxidative stress in arterial hypertension: role of NAD(P)H oxidase. Hypertension 2001;38: 1395–9.
[4] Sorescu D, Weiss D, Lassegue B, et al. Superoxide production and expression of nox family proteins in human atherosclerosis. Circulation 2002;105:1429–35.
[5] Spiekermann S, Landmesser U, Dikalov S, et al. Electron spin resonance characterization of vascular xanthine and NAD(P)H oxidase activity in patients with coronary artery disease: relation to endothelium-dependent vasodilation. Circulation 2003;107:1383–9.
[6] Rey FE, Li XC, Carretero OA, Garvin JL, Pagano PJ. Perivascular superoxide anion contributes to impairment of endothelium-dependent relaxation: role of gp91(phox). Circulation 2002;106:2497–502.
[7] Pratico D, Tangirala RK, Rader DJ, Rokach J, FitzGerald GA. Vitamin E suppresses isoprostane generation in vivo and reduces atherosclerosis in ApoE-deficient mice. Nat Med 1998;4:1189–92.
[8] Fennell JP, Brosnan MJ, Frater AJ, et al. Adenovirus-mediated overexpression of extracellular superoxide dismutase improves endothelial dysfunction in a rat model of hypertension. Gene Ther 2002; 9:110–7.
[9] Unger T. Blood pressure lowering and renin–angiotensin system blockade. J Hypertens 2003;6:S3–7.
[10] Scribner AW, Loscalzo J, Napoli C. The effect of angiotensin-converting enzyme inhibition on endothelial function and oxidant stress. Eur J Pharmacol 2003;482:95–9.
[11] Akishita M, Shirakami G, Iwai M, et al. Angiotensin converting enzyme inhibitor restrains inflammation-induced vascular injury in mice. J Hypertens 2001;19:1083–8.
[12] Antony I, Lerebours G, Nitenberg A. Angiotensin-converting enzyme inhibition restores flow-dependent and cold pressor test-induced dilations in coronary arteries of hypertensive patients. Circulation 1996;94:3115–22.
[13] Warnholtz A, Nickenig G, Schulz E, et al. Increased NADH-oxidase-mediated superoxide production in the early stages of atherosclerosis: evidence for involvement of the renin–angiotensin system. Circulation 1999;99:2027–33.
[14] Choy JC, Granville DJ, Hunt DW, McManus BM. Endothelial cell apoptosis: biochemical characteristics and potential implications for atherosclerosis. J Mol Cell Cardiol 2001;33:1673–90.
[15] Dimmeler S, Haendeler J, Zeiher AM. Regulation of endothelial cell apoptosis in atherothrombosis. Curr Opin Lipidol 2002;13:531–6.
[16] Akishita M, Kozaki K, Eto M, et al. Estrogen attenuates endothelin-1 production by bovine endothelial cells via estrogen receptor. Biochem Biophys Res Commun 1998;251:17–21.
[17] Dimmeler S, Haendeler J, Nehls M, Zeiher AM. Suppression of apoptosis by nitric oxide via inhibition of interleukin-1beta-converting enzyme (ICE)-like and cysteine protease protein (CPP)-32-like proteases. J Exp Med 1997;185:601–7.
[18] Grethe S, Ares MP, Andersson T, Porn-Ares MI. p38 MAPK mediates TNF-induced apoptosis in endothelial cells via phosphorylation and downregulation of Bcl-x(L). Exp Cell Res 2004;298:632–42.
[19] Johnson GL, Lapadat R. Mitogen-activated protein kinase pathways mediated by ERK, JNK, and p38 protein kinases. Science 2002; 298:1911–2.
[20] Cross TG, Scheel-Toellner D, Henriquez NV, Deacon E, Salmon M, Lord JM. Serine/threonine protein kinases and apoptosis. Exp Cell Res 2000;256:34–41.
[21] Rueckschloss U, Quinn MT, Holtz J, Morawietz H. Dose-dependent regulation of NAD(P)H oxidase expression by angiotensin II in human endothelial cells: protective effect of angiotensin II type 1 receptor blockade in patients with coronary artery disease. Arterioscler Thromb Vasc Biol 2002;22:1845–51.
[22] Landmesser U, Cai H, Dikalov S, et al. Role of p47(phox) in vascular oxidative stress and hypertension caused by angiotensin II. Hypertension 2002;40:511–5.
[23] Higashi Y, Sasaki S, Nakagawa K, Matsuura H, Oshima T, Chayama K. Endothelial function and oxidative stress in renovascular hypertension. N Engl J Med 2002;346:1954–62.
[24] Varin R, Mulder P, Tamion F, et al. Improvement of endothelial function by chronic angiotensin-converting enzyme inhibition in heart

failure: role of nitric oxide, prostanoids, oxidant stress, and bradykinin. Circulation 2000;102:351–6.
[25] Onozato ML, Tojo A, Goto A, Fujita T, Wilcox CS. Oxidative stress and nitric oxide synthase in rat diabetic nephropathy: effects of ACEI and ARB. Kidney Int 2002;61:186–94.
[26] de Cavanagh EM, Piotrkowski B, Basso N, et al. Enalapril and losartan attenuate mitochondrial dysfunction in aged rats. FASEB J 2003;17:1096–8.
[27] Hornig B, Landmesser U, Kohler C, et al. Comparative effect of ace inhibition and angiotensin II type 1 receptor antagonism on bioavailability of nitric oxide in patients with coronary artery disease: role of superoxide dismutase. Circulation 2001;103:799–805.
[28] Kofler S, Nickel T, Weis M. Role of cytokines in cardiovascular diseases: a focus on endothelial responses to inflammation. Clin Sci (Lond) 2005;108:205–13.
[29] Shakibaei M, Schulze-Tanzil G, Takada Y, Aggarwal BB. Redox regulation of apoptosis by members of the TNF superfamily. Antioxid Redox Signal 2005;7:482–96.
[30] Griendling KK, Sorescu D, Lassegue B, Ushio-Fukai M. Modulation of protein kinase activity and gene expression by reactive oxygen species and their role in vascular physiology and pathophysiology. Arterioscler Thromb Vasc Biol 2000;20:2175–83.
[31] Huot J, Houle F, Rousseau S, Deschesnes RG, Shah GM, Landry J. SAPK2/p38-dependent F-actin reorganization regulates early membrane blebbing during stress-induced apoptosis. J Cell Biol 1998; 143:1361–73.
[32] Chen K, Vita JA, Berk BC, Keaney Jr JF. c-Jun N-terminal kinase activation by hydrogen peroxide in endothelial cells involves SRC-dependent epidermal growth factor receptor transactivation. J Biol Chem 2001;276:16045–50.
[33] Thomas SR, Chen K, Keaney Jr JF. Hydrogen peroxide activates endothelial nitric-oxide synthase through coordinated phosphorylation and dephosphorylation via a phosphoinositide 3-kinase-dependent signaling pathway. J Biol Chem 2002;277:6017–24.
[34] Shi Y, Gaestel M. In the cellular garden of forking paths: how p38 MAPKs signal for downstream assistance. Biol Chem 2002;383: 1519–36.
[35] Nakagami H, Morishita R, Yamamoto K, et al. Phosphorylation of p38 mitogen-activated protein kinase downstream of bax-caspase-3 pathway leads to cell death induced by high D-glucose in human endothelial cells. Diabetes 2001;50:1472–81.
[36] Takahashi M, Okazaki H, Ogata Y, Takeuchi K, Ikeda U, Shimada K. Lysophosphatidylcholine induces apoptosis in human endothelial cells through a p38-mitogen-activated protein kinase-dependent mechanism. Atherosclerosis 2002;161:387–94.

Microbiol. Immunol., 49(12), 1075–1081, 2005

Editor-Communicated Paper

Analysis of the Distribution of Neuropathogenic Retroviral Antigens Following PVC211 or A8-V Infection

Ryuhei Nakai[1], Sayaka Takase-Yoden[2], and Rihito Watanabe*[,2]

[1]*Department of Geriatric Medicine, Kyorin University School of Medicine, Mitaka, Tokyo 181–8611, Japan, and* [2]*Department of Bioinformatics, Faculty of Engineering, Soka University, Hachioji, Tokyo 192–8577, Japan*

Communicated by Dr. Hiroshi Kida: Received September 14, 2005. Accepted October 6, 2005

Abstract: **A8-V and PVC211 are neuropathogenic strains of the Friend murine leukemia virus (Fr-MLV) that cause spongiosis in the rat brain after infection at birth. PVC211 exhibited stronger neuropathogenicity than A8-V, and induced more severe neurological symptoms such as hind-leg paralysis. These symptoms correlated with the neuropathological spread and intensity, which were more severe in the spinal cord of rats infected with PVC211 than in those infected with A8-V, without exhibiting neuropathological differences in other areas of the CNS. Interestingly, virus titers recovered from infected spinal cords were similar in PVC211 and A8-V infected animals. However, in the spinal cord infected with PVC211, glial cells attained higher immunohistochemical expression scores for the viral surface antigen, gp70 (Env) than in the A8-V infected spinal cord, although expression levels of viral antigens in blood vessel walls were similar in A8-V and PVC211 infections. Furthermore, many of those glial cells which carried viral antigens were found, by double immunostaining, to be microglia. The results suggested that the spread of viral antigen positive microglia plays an important role in forming the different neuro-pathogenicity observed in A8-V and PVC211 infections.**

Key words: **Ecotropic, Histochemistry, CNS**

The FrC6-V, from which A8-V was molecularly cloned (15), and the PVC211 (5) were separately isolated by different methods (20) from the same source of the Fr-MLV complex which had been maintained by mouse-to-mouse passages for over 30 times (10). The A8-V shares a high degree of homology with PVC211 in the R (98.5%), U5 (100%), 5′ leader (99.6%), *gag* (99.6%), pol (99.5%), and env (99.7%) regions (15). The lowest degree of homology between the A8 virus and PVC211 is in the U3 region of the LTR (81.4%). This low homology was attributed to differences in enhancer elements in the U3 region (15). But our recent study using recombinant viruses revealed that the enhancer elements of the neuropathogenic viruses do not contribute to their neuropathogenicity (19), although A8-V enhancer elements appeared to be responsible for its ability to proliferate at high rates in the CNS and to induce tumorigenesis in the thymus and spleen (18).

One common feature of A8-V and PVC211 is that the primary determinant for the induction of neurodegenerative disease is the env gene, but other viral genes also have effects on neuropathogenicity (15). The 0.3-kb fragment containing 0.04-kb of R, U5, and the 5′ half of the 5′ leader of A8 are essential for the induction of spongiform neurodegeneration (19). In the case of PVC211, the sequences within the 5′ leader sequence, the *gag* gene, and the 5′ quarter of the pol gene also influence neurovirulence (9). However, our serial studies using chimerae from A8-V and 57 virus (57-V), the

**Address correspondence to* Dr. Rihito Watanabe, Department of Bioinformatics, Faculty of Engineering, Soka University, Tangi-cho 1–236, Hachioji, Tokyo 192–8577, Japan. Fax: +81–426–91–9465. E-mail: rihito@t.soka.ac.jp

Abbreviations: A8-V, A8 virus; CNS, central nervous system; DAB, 3,3′-diaminobenzidine tetrahydrochloride; EcoR, receptor proteins for ecotropic retroviruses; Env, envelope protein (gp70); 57-V, 57 virus; FrC6-V, FrC6 virus; Fr-MLV, Friend murine leukemia virus; HE, haematoxylin and eosin; MEM, minimum essential medium; NRK, normal rat kidney; PAP, peroxidase-anti-peroxidase; PBS, phosphate-buffered saline; PFU, plaque forming unit.

latter of which is a non-neuropathogenic strain of Fr-MLV proved that the *gag* gene does not need to originate in a neuropathogenic virus in order for a virus to cause neurological disease (16). As part of these studies, we developed recombinant viruses R7c and R7f which lack the enhancer element found in A8-V after the replacement of the fragment with the enhancer element derived from the 57-V gene. These recombinant viruses induced spongiosis with a high incidence, although the isolated viral titers of the infected brain were very low. The mechanism by which viruses with low titers following CNS infection can induce distinct neuropathological lesions was partially revealed by immuno-histochemical studies (21) in which the expression levels of viral antigens following infection with A8-V, R7c, R7f or non-neuropathogenic recombinant virus Rec5 were studied. We employed specific antibodies raised against Env and Gag proteins to evaluate viral antigen expression in blood vessel walls and glia cells in infected brains using the criteria provided in our scoring system. Our data showed that the expression scores of the R7c and R7f viruses were comparable to those of A8-V but distinctly higher than those of Rec5, the latter of which was only minimally expressed in the infected CNS (21).

In this paper, we have compared viral antigen expression levels and neuropathological severity following infection with the A8-V and the PVC211. The main target of A8-V and PVC211 is CNS vascular walls (4, 16), namely endothelial cells (7, 8). The viral antigens in the endothelial cells are distributed not only in or near to the spongiform lesions but also in the areas that appear normal (2, 21). In addition, the viral antigens are not expressed in the neurons of the infected animals although the vacuoles forming spongiosis are located in neuropils (15). The expression levels of Gag and Env proteins assessed after infection with A8-V are identical *in vivo* (21) and *in vitro* (19).

Materials and Methods

Viruses and inoculation. PVC211-producing normal rat kidney cells (NRK) were kindly provided by Dr. Kai (Yamaguchi University, Yamaguchi, Japan). Friend murine leukemia virus (Fr-MLV) clone A8-V was obtained from the virus FrC6-V as described previously (15). Viral titers were determined by the XC cell plaque assay using C182 cells (14) in the presence of 10 μg/ml of Polybrene (14). C182 cells were grown on minimum essential medium (MEM) supplemented with 10% calf serum.

The ability of the viruses to cause disease was assessed using newborn Lewis rats purchased from a commercial breeder. Newborn rats were inoculated by intra-peritoneal (0.1 ml) and intra-cerebral (0.0005 ml) routes with viral supernatant ($1–30\times10^4$ XC-PFU/head). Infected animals were then exsanguinated under deep anesthesia and the dissected organs were homogenized in cold phosphate-buffered saline (PBS) containing 1 mM $MgCl_2$ and 1 mM $CaCl_2$. Infectious virus titers were then determined by the XC cell plaque assay (14).

Histology. Following exsanguination of the animals 6–7 weeks after infection, the collected organs were immersed and fixed in 4% paraformaldehyde buffered with 0.12 M phosphate (pH 7.3). Tissues were then embedded in paraffin for histological staining with haematoxylin and eosin (HE).

The degree of spongiform neurodegeneration was scored as follows: 0—no lesions; 1—less than 20 vacuoles in the total area; 2—20 to 100 vacuoles counted in the light microscopical field at 10× magnification (field (×10)); 3—clusters consisting of over 100 vacuoles spread within one field (×10); 4—more than two clusters consisting of over 100 vacuoles in the area, or clusters of vacuoles occupying over 30% of the total area. Intermediate scoring in between each of the seven established scores was permitted by adding a value of 0.5 to the lower score. To score CNS pathology, five areas were selected: cerebral cortex, thalamus, cerebellum, pons and spinal cord.

For detection of the viral antigen proteins Env and Gag, we performed immunohistochemistry using goat anti-Rauscher MLV gp70 (antiEnv) (Quality Biotech Incorporated Resource Laboratory) and anti-AKR $p30^{Gag}$ (antiGag, Quality Biotech Incorporated Resource Laboratory) on thin paraffin sections (2). Non-specific antibody binding was blocked by incubation of sections and cells with 50% normal mixed serum (fetal calf, calf, pig, and horse) diluted in PBS. Biotinylated rabbit anti-goat IgG (ZYMED Laboratories, Inc.) was used as a secondary antibody followed by treatment with an avidin-peroxidase complex (ZYMED Laboratories, Inc.). Washes in PBS were carried out between each step. After primary antibody incubation, the non-specific activity of endogenous peroxidase activity was blocked by incubating cells with 0.3% H_2O_2 in methanol. For the peroxidase reaction, 0.2 mg/ml 3,3′-diaminobenzidine tetrahydrochloride (DAB) (DOTIDE) in 0.1 M Tris buffer (pH 7.6) was used. In order to confirm that most of the glial cells carrying viral antigens are microglia, double immunostaining was carried. ED-1 monoclonal antibody was used to detect microglia as primary antibody (22). The antiGag reaction was developed first using the PAP method and donkey anti-goat IgG (Bethyl Lab., Inc.), peroxidase labeled goat IgG (DACO), and DAB, to yield a brown

reaction product. ED-1 was visualized using 20 mg/ml of 4-chloro-1-naphtol (WAKO, Japan), which gave a purple reaction product after sequential application of biotinylated rabbit anti-mouse antibody (ZYMED Laboratories, Inc.) and an avidin-peroxidase complex (ZYMED Laboratories, Inc.). Nuclei were counterstained with methyl green.

The intensities of antigen expression were scored separately either in blood vessels or in glial cells of the CNS. Scoring was performed in the same areas used for pathological evaluation. The degree of antigen expression in the blood vessels was scored as follows: 0—no antigens; 1—less than 10% of antigen-positive blood vessels in the sample area; 2—10–20% antigen-positive blood vessels in the sample area; 3—20–50% antigen-positive blood vessels in the sample area; 4—more than 70% antigen-positive blood vessels in the sample area. The degree of antigen expression in glial cells was scored as follows: 1—a few antigen-positive glial cells in total area; 2—more than 10 antigen-positive glial cells in the field at 10× magnification (field (×10)); 3—more than three fields (×10) that contain more than 10 antigen-positive glial cells; 4—fields with more than 10 antigen-positive glial cells occupy more than 70% of the area.

Results

Clinical Sign

None of the 10 rats that were infected with A8-V developed hind-leg paralysis or weakness within 6 weeks after inoculation and three out of ten infected rats manifested hind-leg paralysis afterwards. Three rats infected with A8-V did not show any neurological signs over the course of 8 weeks post inoculation. In contrast, half of the PVC211 infected rats developed hind-leg weakness within 6 weeks of inoculation and most (11/12 infected rats) manifested hind-leg paralysis by 8 weeks post inoculation.

Virus Growth

The virus titers recovered from the brains and spinal cords 6–7 weeks after infection with the A8-V ranged $3–50\times10^4$ and $9–60\times10^4$, respectively. The averages obtained from five infected rats were 1.8×10^5 and 3.4×10^5 respectively (Fig. 1). The infection of the PVC211 induced similar level of viral recovery from the brain and the spinal cord at 6–7 weeks post inoculation ranging from $1.3–3.7\times10^4$ and $4.8–7.2\times10^4$, respectively. The averages obtained from four rats infected with PVC211 were 3.0×10^4 and 6.1×10^4 respectively.

Histopathology

The degree of spongiotic change induced by the infection was assessed by a scoring system (see "Materials and Methods") after evaluation of 5 areas (cerebral cortex, thalamus, cerebellum, pons, and spinal cord) of each infected animal. A typical spongiosis scored as 3 is shown in Fig. 2. There, the HE staining illustrates many vacuoles with diameters of 5–100 μm compose a fairly well demarcated area of spongiosis (Fig. 2A). The average scores obtained from the spinal cords of 7 rats infected with the A8-V and 3 rats infected with PVC211 were 1.4 and 2.8, respectively (Fig. 1), suggesting that PVC211 induced more severe neuropathology in the spinal cord compared to A8-V ($P<0.002$ by Student's test). The average neuropathological scores in the cerebral cortex, thalamus, pons, and cerebellum (designated cumulatively as Brain in Fig. 1) were similar in PVC211 and A8-V infected rats ($P>0.7$).

Histochemistry

Viral antigens were detected predominantly in the vascular walls of infected brains regardless of the virus used (Fig. 2E), and with the exception of the vascular wall, were detected at lower frequencies in glial cell structures (Fig. 2, C and F). The glial structures associated with viral antigens were regularly encountered close to and inside spongiotic lesions and were often attached to the wall of the vacuole (Fig. 2C). On the other hand, virus-expressing blood vessels exhibited a much wider distribution, and were often found in the regions where no spongiosis was observed (Fig. 2E).

This closer correlation of antigen expression to the lesions in glial cells than in vascular walls was statistically analyzed. The expression levels of the Env protein were evaluated according to our evaluation score (see "Materials and Methods"), examined in selected five areas within the CNS as described earlier for a pathological scoring system. When the expression levels of the viral antigen in the glial cells (env/glia in Fig. 1) activated in the spinal cords were compared between PVC211 and A8-V infection, PVC211 infection induced more than twice the levels of antigen expression in glial cells compared to A8-V ($P<0.04$). In contrast, no significant difference was observed in the expression of Env protein in the vascular walls following infection by these viruses (env/vessel in Fig. 1) in the spinal cord ($P>0.3$). Furthermore, there also was no significant difference in the env/glia immunohistochemical scores obtained from the brain (cerebral cortex, thalamus, pons, and cerebellum, designated as Brain in Fig. 1) between the PVC211 and A8-V infected groups ($P>0.4$).

In order to confirm the previous report that spongi-

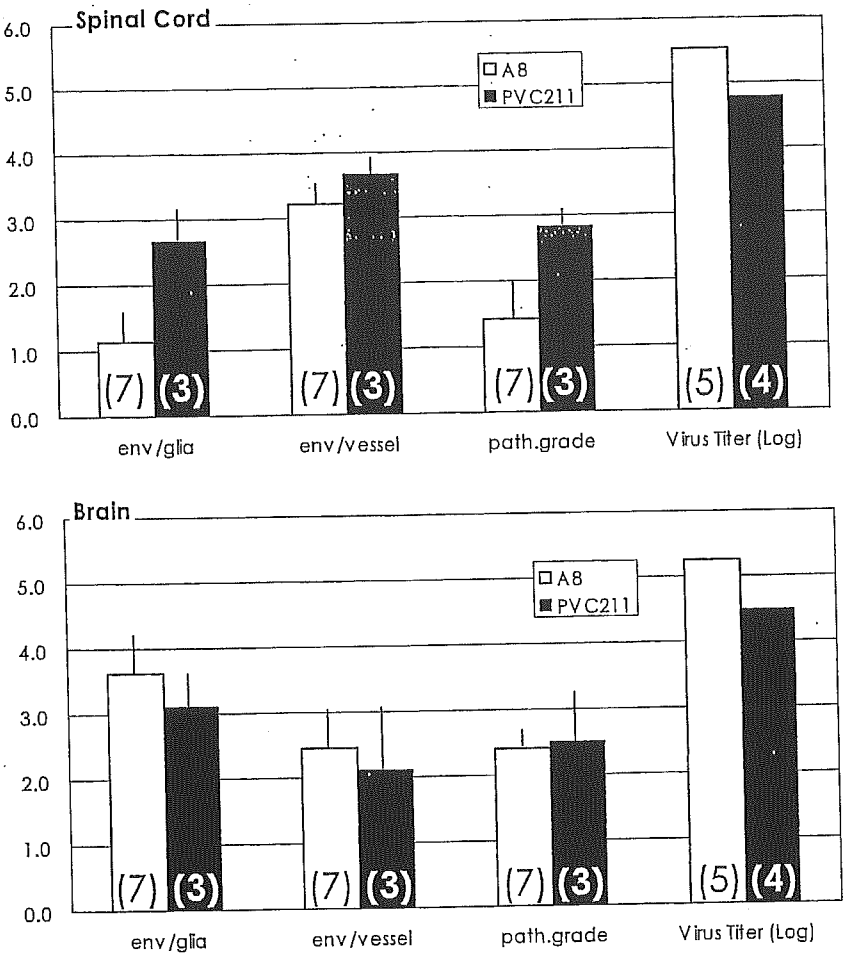

Fig. 1. Histological scores and viral growth. Numbers in the parentheses described in the bars indicate the numbers of rats examined. Env expression estimated by immuno-histochemistry either in the blood vessel wall or glia cells is described as Env/vessel or glia, respectively, and the pathological grade as path. grade. The immunohistochemical and pathological scores of each animal was evaluated by the averaging the data obtained from spinal cord or brain which is investigated in 4 different areas (cerebral cortex, thalamus, cerebellum, and pons).

form degenerations induced by several neuropathogenic murine retroviruses are associated primarily with infection of microglial cells (13), we performed double immunostaining. Our data showed that many of the glial cells that bore viral antigen (Fig. 2F) also expressed a microglial marker protein that was identified by the monoclonal antibody ED-1 (Fig. 2F).

Discussion

Our data showed that PVC211 was more neuropathogenic in neonatal rats than A8-V, as manifested by the higher incidence and more rapid onset of hind-leg paralysis in these animals. This neurological sign was due to the presence of pathological lesions in the spinal cord, which have also been investigated in other neurological diseases which are experimentally induced in rats, such as experimental allergic encephalomyelitis (2). Our neuropathological data confirmed the presence of viral lesions in the spinal cord of rats that developed paralysis and, as expected based on our neurological findings, rats that were infected with PVC211 showed more of such lesions.

The above data notwithstanding, viral titers recovered from the spinal cords of PVC211 and A8-V infected rats were similar (Fig. 1). From a virological view point, it has been considered that the level of viral titer obtained from a target organ is correlated to pathological severity in the relevant organs (11, 13, 14). However, our recent studies using chimeric viruses derived from the genes of A8-V and a non-neuropathogenic Fr-MLV, 57-V revealed that neuropathology induced by A8-V infection is not dependent upon the viral proliferation rate but rather the level of viral antigen expression (19). Nevertheless, this comparative study using chimerae resulted in a comparison between neuropathogenic and

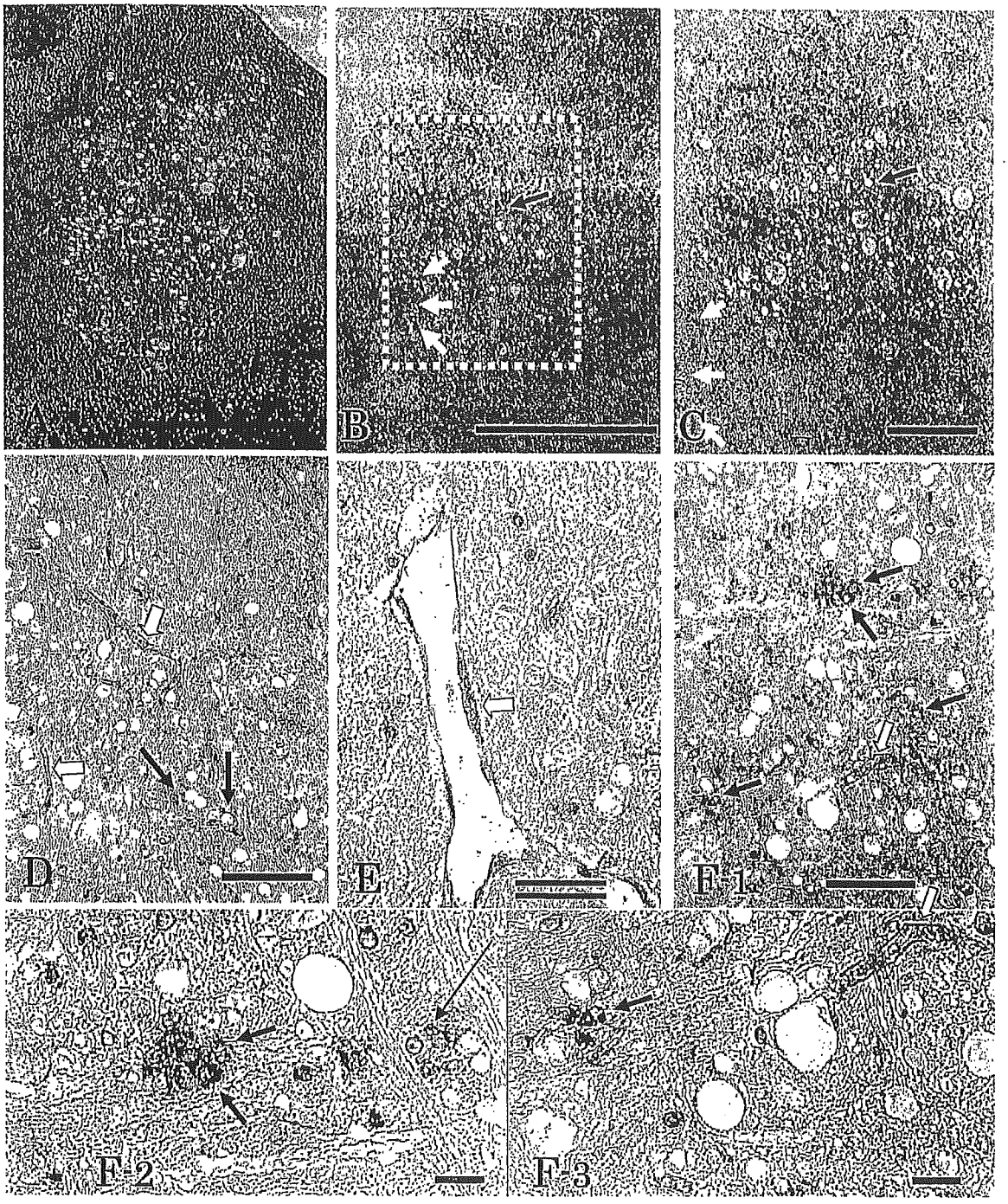

Fig. 2. Histology after infection. HE staining (A) and immuno-histochemistry (B–E) using anti-Gag or anti-Env protein antibodies (designated as Gag or Env in each photograph respectively) 8 weeks after infection with A8-V or PVC211. The inoculated virus is indicated in each photograph. A–D: Areas around the lateral cerebellar nucleus stained for serial sections. The black arrows indicate glial cells bearing viral antigen which attach to the vacuolar wall while the white arrows indicate the antigen-positive blood vessels. The rectangular region in figure B is shown at higher magnification in C. The expression levels of Env (C) and Gag proteins (D) were similar as we previously reported (in press). E: Note the antigen-positive blood vessel indicated by the white arrow in the area of normal appearance. F: Double immunostaining for Gag protein (brown color) and a microglial marker protein (purple color). Pictures taken at higher magnification of F-1 are shown in F-2 and F-3. Note the viral antigen-positive blood vessel (brown staining) at the white arrow and the double labeled microglial cells staining brown and purple at the bolded black arrows. The long black arrow indicates a positively stained (purple) uninfected microglial cell. The single bars and double lines indicate 500 μm and 125 μm, respectively.

non-neuropathogenic chimerae, and the viral antigen expression in blood vessel walls of the CNS infected with non-neuropathogenic chimerae was also suppressed as well as in glial cells (19). Therefore, the significance of viral antigen positive glial cells in forming spongiotic lesions could not be evaluated in the comparative study mentioned above.

We have proposed that glial cells carrying viral antigens might contribute to developing neuropathological lesions induced by A8-V infection, because we often observe the antigen positive glial cells attaching to the walls of vacuoles which compose spongiotic lesions (17, 21). In addition, numerous reports have suggested that spongiform degeneration induced by neuropathogenic murine retroviruses is primarily associated with infection of microglial cells (1, 3, 6, 12). The results of our double labeling study confirmed that A8-V infection also induces many microglial cells which carry viral antigens (Fig. 2F). However, the importance of the suggested association of infected microglia with neuropathological lesions remains unknown, because viral antigen positive blood vessel walls are encountered in much higher frequency than viral antigen positive microglia in infected CNS (4, 7, 17, 20), and no statistical analysis had been done until now. In this paper, we clarified that viral antigen positive microglial cells were really associated with lesional distribution after a statistical analysis. Furthermore, distribution of antigen positive blood vessels was proved not to be statistically correlated with that of neuropathological lesions. Neuropathological changes induced by infections of A8-V and PVC211, which share a common genetical background, were almost identical except for the intensity of lesions in spinal cords, where similar levels of viral antigen expression in blood vessel walls were obtained from those viral infections. It is not clear how PVC211 induced a higher population of infected microglial cells in infected spinal cords than A8-V, in spite of the fact that these two viruses exhibit similar viral titers in brains and in spinal cords as well. The difference in the infectivity of the two viruses to glial cells in spinal cords might be due to different proliferation rates of these viruses during an earlier period of infection than the time when we compared the outcome at 6–8 weeks after infection, because the viral titers recovered from the CNS infected with A8-V at the newborn stage reach a plateau at 3–4 weeks after infection (15). And the expression levels of the receptor proteins for ecotropic retroviruses (EcoR) in rat brains change at the age of 4–5 weeks (17). We molecularly cloned the EcoR gene from F10 cells (F10-EcoR) (16), which are derived from rat glial cells. Application of a specific antibody for F10-EcoR protein visualized, by an immunohistochemical procedure, the F10-EcoR protein expression both in blood vessel walls and in glial cells of the CNS (16). The expression level of the F10-EcoR protein in rat glial cells reduced dramatically at the age of 4 weeks old, while that in the blood vessel walls of the rat CNS was well maintained afterwards (17). Although a close association of viral antigen positive microglial cell with lesional distribution was indicated, we still do not have any evidence or information as to whether those antigen positive microglial cells really create the vacuoles in the neuropils.

The authors thank Katsumi Goto for performing the histological studies. This work was supported in part by a Grant-in-Aid for Scientific Research from the Japan Society for the Promotion of Science and "High-Tech Research Center" Project for Private Universities: matching fund subsidy from MEXT, 2004–2008.

References

1) Baszler, T.V., and Zachary, J.F. 1991. Murine retroviral neurovirulence correlates with an enhanced ability of virus to infect selectively, replicate in, and activate resident microglial cells. Am. J. Pathol. **138**: 655–671.
2) Fukumitsu, H., Takase-Yoden, S., and Watanabe, R. 2002. Neuro-pathology of experimental autoimmune encephalomyelitis modified by retroviral infection. Neuropathology **22**: 280–289.
3) Gravel, C.D., Kay, G., and Jolicoeur, P. 1993. Identification of the infected target cell type in spongiform myeloencephalopathy induced by the neurotropic Cas-Br-E murine leukemia virus. J. Virol. **67**: 6648–6658.
4) Ikeda, T., Takase-Yoden, S., and Watanabe, R. 1995. Characterization of monoclonal antibodies recognizing neurotropic Friend murine leukemia virus. Virus Res. **38**: 297–304.
5) Kai, K., and Furuta, T. 1984. Isolation of paralysis-inducing murine leukemia viruses from Friend virus passaged in rats. J. Virol. **50**: 970–973.
6) Lynch, W.P., Robertson, S.J., and Portis, J.L. 1995. Induction of focal spongiform neurodegeneration in developmentally restricted mice by implantation of murine retrovirus-infected microglia. J. Virol. **69**: 1408–1419.
7) Masuda, M., Hanson, C.A., Dugger, N.V. et al. 1997. Capillary endothelial cell tropism of PVC-211 murine leukemia virus and its application for gene transduction. J. Virol. **71**: 6168–6173.
8) Masuda, M., Kakushima, N., Wilt, S.G. et al. 1999. Analysis of receptor usage by ecotropic murine retroviruses, using green fluorescent protein-tagged cationic amino acid transporters. J. Virol. **73**: 8623–8629.
9) Masuda, M., Remington, M.P., Hoffman, P.M., and Ruscetti, S.K. 1992. Molecular characterization of a neuropathogenic and nonerythroleukemogenic variant of Friend murine leukemia virus PVC-211. J. Virol. **66**: 2798–2806.
10) Odaka, T., Ikeda, H., Yoshikura, H., Moriwaki, K., and

Suzuki, S. 1981. Fv-4: gene controlling resistance to NB-tropic Friend murine leukemia virus. Distribution in wild mice, introduction into genetic background of BALB/c mice, and mapping of chromosomes. J. Natl. Cancer Inst. **67**: 1123–1127.

11) Portis, J.L. 2001. Genetic determinants of neurovirulence of murine oncornaviruses. Adv. Virus Res. **56**: 3–38.
12) Portis, J.L., Czub, S., Garon, C.F., and McAtee, F.J. 1990. Neurodegenerative disease induced by the wild mouse ecotropic retrovirus is markedly accelerated by long terminal repeat and gag-pol sequences from nondefective Friend murine leukemia virus. J. Virol. **64**: 1648–1656.
13) Portis, J.L., Czub, S., Robertson, S., McAtee, F., and Chesebro, B. 1995. Characterization of a neurologic disease induced by a polytropic murine retrovirus: evidence for differential targeting of ecotropic and polytropic viruses in the brain. J. Virol. **69**: 8070–8075.
14) Rosenberg, N., and Jolicoeur, P. 1997. Retroviral pathogenesis, p. 475–585. *In* Coffin, J.M., Hugbes, S.H., and Varmus, H.E. (eds), Retriviruses, Cold Spring Harbor Laboratory Press, New York.
15) Takase-Yoden, S., and Watanabe, R. 1997. Unique sequence and lesional tropism of a new variant of neuropathogenic Friend murine leukemia virus. Virology **233**: 411–422.
16) Takase-Yoden, S., and Watanabe, R. 1999. Contribution of virus-receptor interaction to distinct viral proliferation of neuropathogenic and nonneuropathogenic murine leukemia viruses in rat glial cells. J. Virol. **73**: 4461–4464.
17) Takase-Yoden, S., and Watanabe, R. 2001. Distribution of ecotropic retrovirus receptor protein in rat brains detected by immunohistochemistry. J. Gen. Virol. **82**: 1815–1820.
18) Takase-Yoden, S., and Watanabe, R. 2002. Identification of genetic determinants that regulate tumorigenicity of Friend murine leukemia virus in rats. Microbiol. Immunol. **46**: 885–890.
19) Takase-Yoden, S., and Watanabe, R. 2005. A 0. 3 kb fragment containing the R-U5-5′ leader sequence is essential for the induction of spongiform neurodegeneration by A8 murine leukemia virus. Virology **336**: 1–10.
20) Watanabe, R., and Takase-Yoden, S. 1995. Gene expression of neurotropic retrovirus in CNS. Prog. Brain Res., **105**: 255–262.
21) Watanabe, R., and Takase-Yoden, S. 2005. Neuropathology induced by infection with Friend murine leukemia clone A8-V depends upon the level of viral antigen expression. Neuropathology (in press).
22) Watanabe, R., Takase-Yoden, S., Fukumitsu, H., and Nakajima, K. 2002. Cell transplantation to the brain with microglia labeled by neuropathogenic retroviral vector system. Cell Transplant. **11**: 471–473.